

**Supporting Information for:**

Surface Heterogeneity on Hemispheres-in-Cell Model Yields All  
Experimentally-observed Non-Straining Colloid Retention Mechanisms in  
Porous Media in the Presence of Energy Barriers

Huilian Ma, Eddy Pazmino, William P. Johnson\*

Department of Geology and Geophysics

University of Utah, Salt Lake City, UT 84112

Total pages: 12 including this cover page

Text: 8

Figures: 4

---

\* Corresponding author. Email: [William.johnson@utah.edu](mailto:William.johnson@utah.edu); Tel: (801)585-5033; Fax: (801)581-7065.

## **Discretization scheme and GSI force integration**

Colloid and collector surfaces were discretized into small surface area elements in a way that the projected area from every element onto the plane perpendicular to the line connecting the colloid center to the hemisphere center was kept constant, as illustrated in [Figure S1](#). In this work, the size of heterodomains was set equal to the size of discretized area elements. Typically only a small portion of the colloid's projection on the collector surface would contribute significantly to the overall colloid-surface interaction due to the curvature of colloid (and collector) surface and the rapid decay of colloidal interaction with distance.<sup>1,2</sup> So the force calculation between these interacting area elements was set to start from the center elements (i.e. elements that intersect colloid center-hemisphere center line) and then expand outward to include the surrounding elements via addition of one ring of adjacent elements at a time. For a given colloid surface element, ring expansion from the collector surface would stop if the force contribution from the entire ring was less than 5% of the force from the center plus the first ring ([Figure S1](#)). Ring expansion from the colloid surface would also stop once the number of rings being checked on the colloid surface exceeded the number of rings being checked on the collector surface or outside of the projection of colloid onto the collector surface.

## **Generating heterogeneous domains**

Two strategies were used to generate the positively charged heterogeneous domains

over the spherical collector surfaces. For cases requiring less number of heterodomains (e.g. as a result of low surface coverage or big domain size), all heterodomains (randomly distributed and without overlapping) were generated across the spherical collector surfaces, sorted into multiple sectors based on their respective z coordinates to reduce computational cost, and stored as input for the trajectory model.

For cases requiring large number of heterodomains (e.g. high surface coverage, small domain size), the process of sorting through all stored domains (sectors) to locate relevant ones for GSI force computations became very time consuming; consequently, it slowed down the trajectory simulations, especially when simulating small size colloids. So, instead of pre-generating all required domains, we employed a different approach to probabilistically generate them as colloids move along the collector surface within a distance range that colloidal forces are rendered to be influential (e.g. from secondary energy minimum toward the surface). Since this probabilistic approach only generates heterodomains along the parts of collector surfaces with which colloids will be closely associated, it potentially reduces the number of heterodomains needed to be generated, stored, and sorted through, and as a result it speeds up the simulation process. The way it works is that for every collector surface element, a randomly generated number from 0 to 1 (Gaussian distribution), representing the probability of this element being a heterodomain, is compared to the pre-determined probability corresponding to the desired coverage. If the random number

is less than the calculated probability, this element is designated as a positively charged heterodomain; otherwise, this element remains negatively charged. The number and locations of thus generated heterodomains were recorded and passed along to all computers (if multiple computers are involved in trajectory simulations) using message passing interface (MPI) algorithms. These heterodomains were always searched first before generating new ones to prevent heterodomain overlapping.

### **Coordinate transformation during GSI implementation**

Implementing the GSI technique in the hemispheres-in-cell model requires accurate identification of heterogeneous domains over the *spherical* collector surface; however, the heterodomain ring expansion as described above often can be easily carried out on a projected *planar* surface. So two Cartesian coordinate systems were used to map the projected (planar) surface elements during the ring expansion to the actual spherical collector surfaces and coordinate transformation was performed between these two coordinate systems.

### **Tangential forces during physical contact**

Following Duffadar and Davis,<sup>1,2</sup> the tangential forces “upon contact” can be summed as follows:

$$m \frac{du_t}{dt} = F_t^{VM} + F_t^G + F_t^B + F_t^{tr} + F_t^r + F_t^s + F_t^{df} + F_t^{rf}, \quad (s1)$$

where  $F_t^{tr}$ ,  $F_t^r$ ,  $F_t^s$  represent the hydrodynamic resistances from translation, rotation, and

fluid shear, respectively;  $F_t^{df}$  ( $= \mu_F F_n$ ) and  $F_t^{rf}$  ( $= \mu_R F_n$ ) are dynamic and rolling friction forces, respectively; all the other parameters are defined in the main manuscript. The explicit expression balancing the tangential forces is shown below where non-drag forces (excepting  $F_t^{VM}$ ) are grouped such that  $F_t^{GRP} = F_t^G + F_t^B$ :

$$m \frac{du_t}{dt} + \frac{4}{3} \pi a_p^3 \frac{1}{2} \rho_f \frac{du_t}{dt} = F_t^{GRP} + F_t^{tr*} 6\pi\mu a_p u_t + F_t^{r*} 6\pi\mu a_p^2 \Omega + F_t^{s*} 6\pi\mu a_p hS + (\mu_F + \mu_R)(F_n) \quad (s2)$$

where  $S$  is shear rate,  $\Omega$  is particle rotational velocity. The torque balance in the tangential direction is:

$$0 = T_y^{tr*} 8\pi\mu a_p^2 u_t + T_y^{r*} 8\pi\mu a_p^3 \Omega + T_y^{s*} 4\pi\mu a_p^3 S - \mu_F (F_n) a_p \quad (s3)$$

Combining equations (s2) and (s3) to eliminate  $\mu_F$  under the assumption that the value of  $\mu_F$  is sufficiently large that rolling (rather than slipping) occurs (following Duffadar and Davis<sup>2</sup>).

Under this condition, the following is also true:  $\Omega a_p = u_t$ . Making this substitution (and also noting  $hS = v_t$ ) yields:

$$m \frac{du_t}{dt} + \frac{4}{3} \pi a_p^3 \frac{1}{2} \rho_f \frac{du_t}{dt} = F_t^{GRP} + F_t^{tr*} 6\pi\mu a_p u_t + F_t^{r*} 6\pi\mu a_p^2 u_t + F_t^{s*} 6\pi\mu a_p hS + (\mu_R)(F_n) + T_y^{tr*} 8\pi\mu a_p u_t + T_y^{r*} 8\pi\mu a_p^2 u_t + T_y^{s*} 4\pi\mu a_p^2 S \quad (s4)$$

Re-arranging yields:

$$\left( m + \frac{2}{3} \pi a_p^3 \rho_f \right) \frac{du_t}{dt} = F_t^{GRP} + \mu_R F_n + 6\pi\mu a_p u_t (F_t^{tr*} + F_t^{r*} a_p + T_y^{tr*} \frac{4}{3} + T_y^{r*} \frac{4}{3} a_p) + 6\pi\mu a_p v_t (F_t^{s*} + T_y^{s*} \frac{2}{3} \frac{a_p}{h}) \quad (s5)$$

Approximating the time differential:

$$\begin{aligned}
\left(m + \frac{2}{3}\pi a_p^3 \rho_f\right) \left(\frac{u_t^\tau - u_t^{\tau-1}}{\Delta t}\right) &= F_t^{GRP,\tau} + \mu_R^\tau F_n^\tau + 6\pi\mu a_p u_t^\tau (F_t^{tr*} + F_t^{r*} a_p + T_y^{tr*} \frac{4}{3} + T_y^{r*} \frac{4}{3} a_p) \\
&\quad + 6\pi\mu a_p v_i^\tau (F_t^{s*} + T_y^{s*} \frac{2}{3} \frac{a_p}{h}) \\
u_t^\tau &= \frac{u_t^{\tau-1} \left(m + \frac{2}{3}\pi a_p^3 \rho_f\right) + F_t^{GRP,\tau} \Delta t + \mu_R^\tau F_n^\tau \Delta t + 6\pi\mu a_p v_i^\tau \Delta t (F_t^{s*} + T_y^{s*} \frac{2}{3} \frac{a_p}{h})}{\left[\left(m + \frac{2}{3}\pi a_p^3 \rho_f\right) - 6\pi\mu a_p \Delta t (F_t^{tr*} + F_t^{r*} a_p + T_y^{tr*} \frac{4}{3} + T_y^{r*} \frac{4}{3} a_p)\right]} \quad (s6)
\end{aligned}$$

where we considered  $F_n$  equal to the colloidal force (not including Brownian and gravitational), since this is the dominant force acting at separation distances closer than the energy barrier maximum.

### Rolling friction coefficient ( $\mu_R$ )

Following Bergendahl and Grasso<sup>3</sup> analysis, the rolling friction coefficient ( $\mu_R$ ) was given by:

$$\mu_R = \beta \frac{2a_{contact}}{3\pi a_p} \quad (s7)$$

where  $\beta$  is the hysteresis loss factor (approximated with the value of  $1.55 \times 10^{-3}$ , as in Johnson's work<sup>4</sup>, but we understand that this hysteresis loss factor is material dependent and highly variable); and  $a_{contact}$  is the radius of the contact area between the interacting colloid and surface, given by

$$a_{contact} = \left(0.63 \frac{6W\pi a_p^2}{K}\right)^{\frac{1}{3}} \quad (s8)$$

where  $W$  is the interaction energy per unit area ( $J/m^2$ ), approximated by the interaction energy at the primary energy minimum, and  $K$  is the composite Young's modulus

(approximated with the value of  $4.014 \times 10^9 \text{ N/m}^2$  as in Bergendahl and Grasso<sup>3</sup> for polystyrene colloidal particles interacting with glass bead collectors).

### Relationship between collector efficiency ( $\eta$ ) and deposition rate constant ( $k_f$ )

The simulated collector efficiency ( $\eta$ ) from the hemispheres-in-cell model is related to the deposition rate constant ( $k_f$ ) as follows:<sup>5</sup>

$$k_f = \frac{3(1-\varepsilon)}{2d_c} \eta v_p \left[ \frac{3-\varepsilon}{3-3\varepsilon} - \frac{2(3-\varepsilon)}{\pi(3-3\varepsilon)} \cos^{-1} \left( \frac{3-3\varepsilon}{3-\varepsilon} \right)^{1/2} + \frac{2}{\pi} \sqrt{2 \left( \frac{3-\varepsilon}{3-3\varepsilon} \right)^{1/2} - 1} \right] \quad (\text{s9})$$

where  $\varepsilon$  is the porosity,  $v_p$  is the average pore water velocity in the model and  $d_c$  is the collector diameter.

### Equations for mean-field DLVO interaction energy

The mean-field DLVO interaction energy ( $\Delta G_{\text{total}} = \Delta G_{\text{FDL}} + \Delta G_{\text{vdW}}$ ) between a colloid and the collector surface was calculated based on the following equations<sup>6,7</sup> (a sphere-plate configuration was used as a result of the size difference between the colloid and the collector). The mean-field DLVO force expressions presented in Appendix A in the main manuscript were given by  $-d(\Delta G)/dh$ . Please see the manuscript for the definitions of parameters used in these equations.

$$\Delta G_{\text{FDL}} = \pi \varepsilon_r \varepsilon_0 a_p \left[ 2 \zeta_p \zeta_c \ln \left( \frac{1 + \exp(-\kappa h)}{1 - \exp(-\kappa h)} \right) + (\zeta_p^2 + \zeta_c^2) \ln(1 - \exp(-2\kappa h)) \right] \quad (\text{s10})$$

$$\Delta G_{\text{vdW}} = -\frac{Ha_p}{6h} \frac{1}{(1 + 11.116h/\lambda)}. \quad (\text{s11})$$

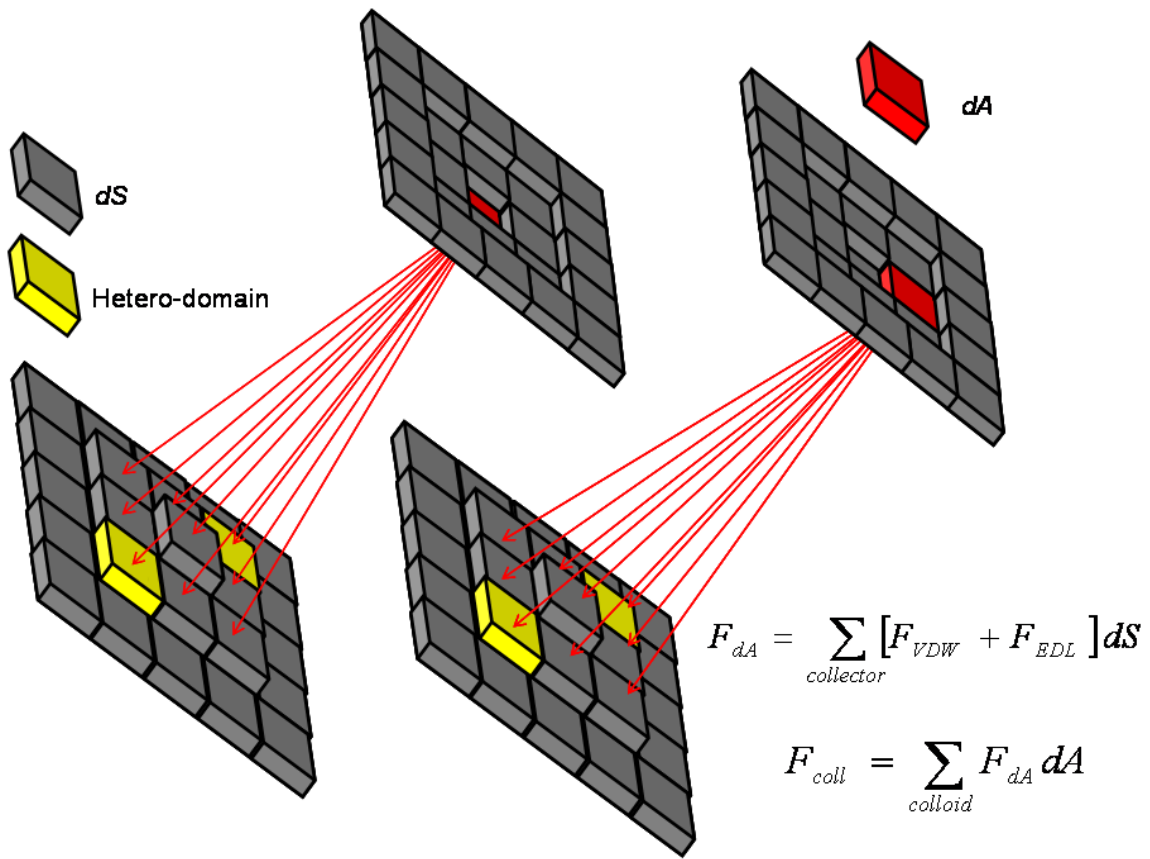


Figure S1. GSI discretization scheme.



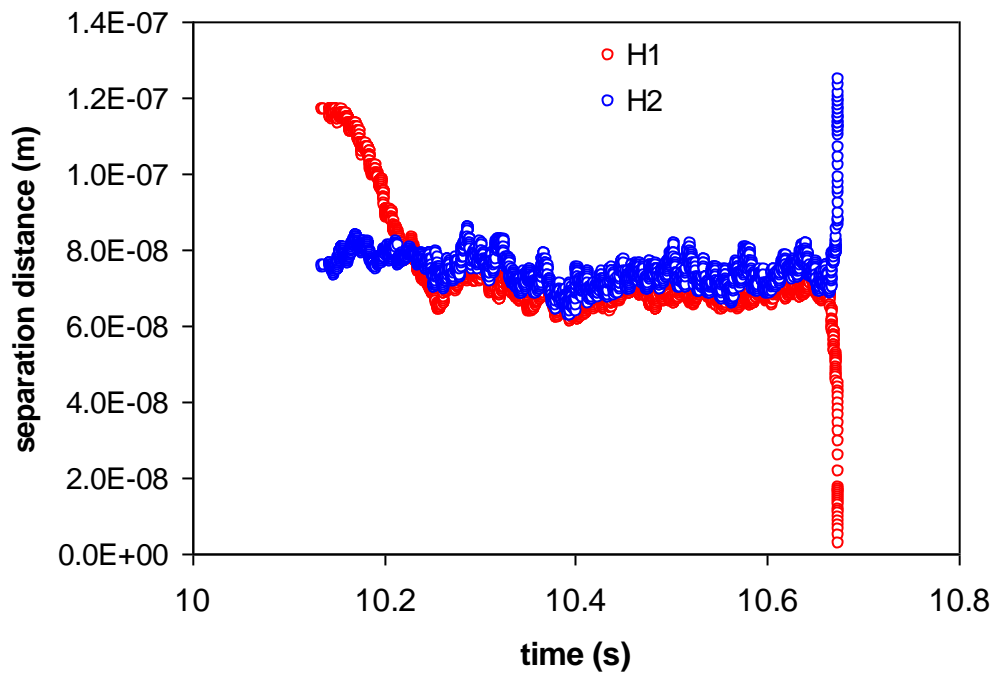


Figure S2. The changes in separation distances between a 10- $\mu\text{m}$  colloid and two collector surfaces (H1 and H2) just before its being wedged at grain to grain contact.

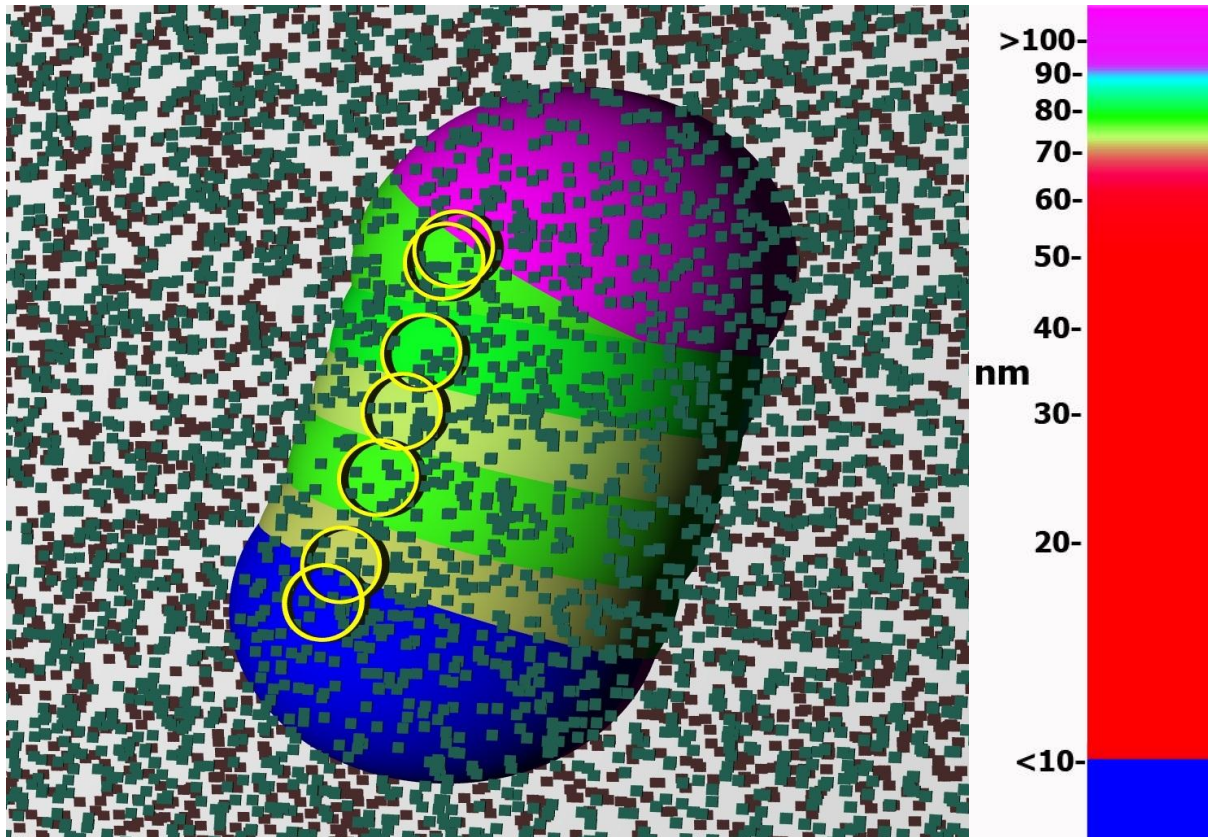


Figure S3. An Image showing the near-surface trajectories (e.g. from secondary energy minimum towards the surface) for a colloid being wedged at grain to grain contact viewed from the inside of the transparent collector it attached, as compared to the view in [Figure 5](#) from the main text. Colloids are rendered in colors to reflect their colloid-collector separation distances as indicated by the color spectrum; and distances corresponding to secondary and primary energy minimum are marked with magenta and blue, respectively. The heterodomains from the collector to which the colloid attached are shown in dark green squares, and the heterodomains from the other collector in dark red squares. The zone of influence (ZOI) is indicated with a yellow circle.

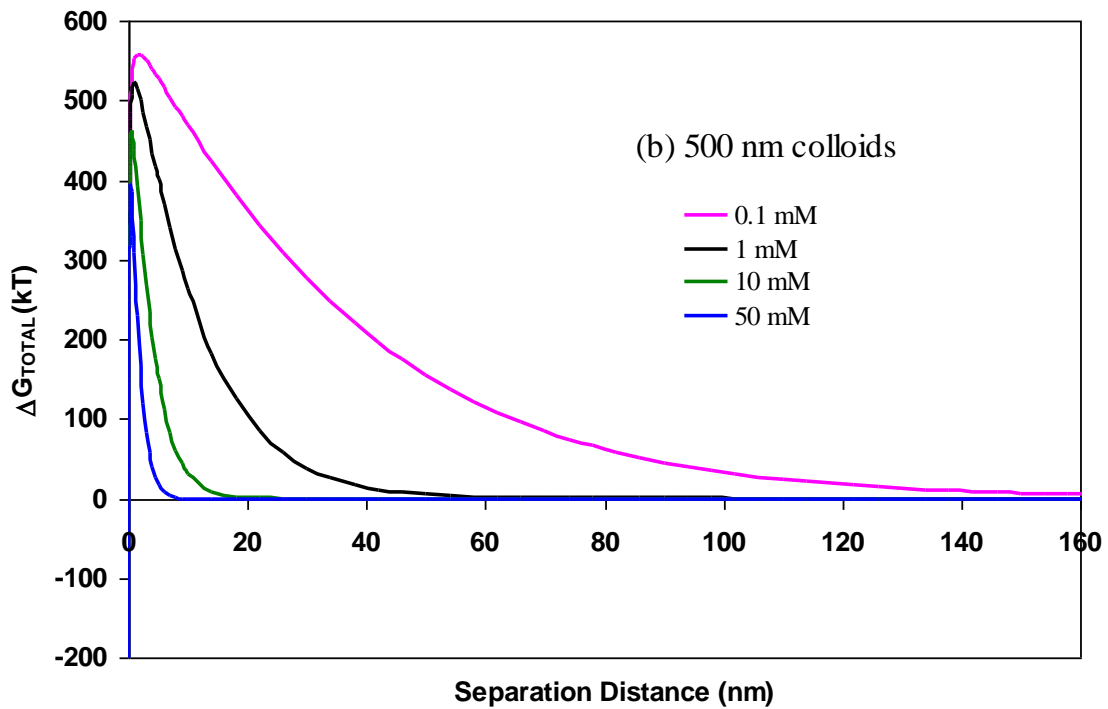
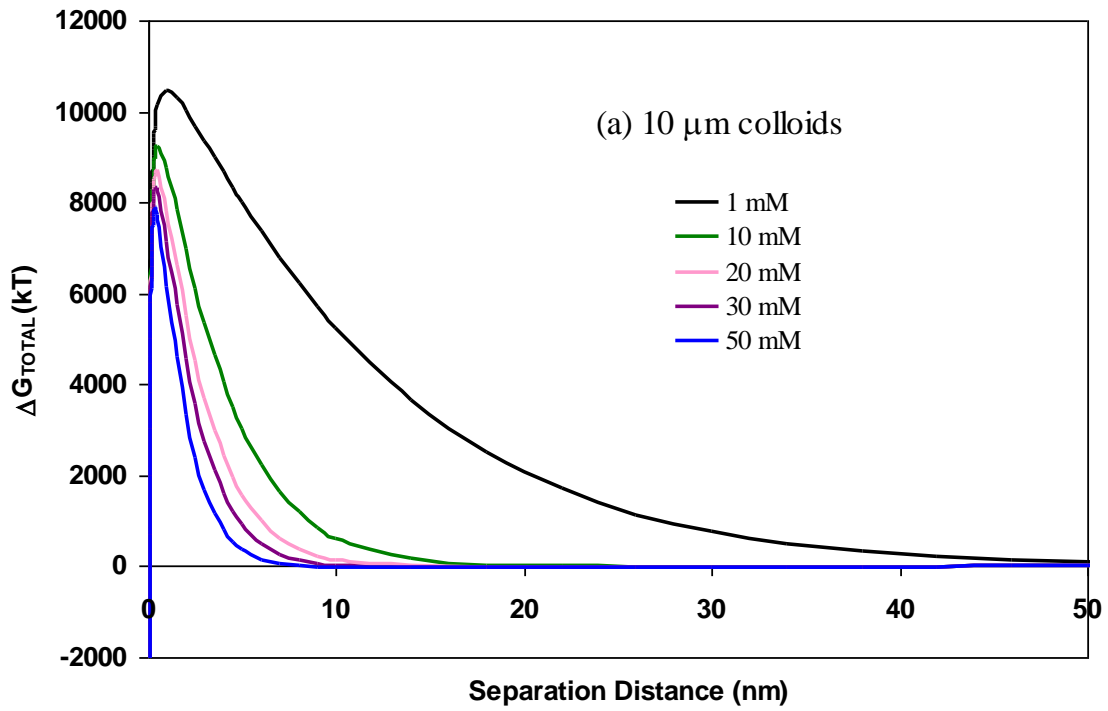


Figure S4. The colloid-surface interaction potential ( $\Delta G$ ) as a function of separation distance calculated from the mean-field DLVO theory (eqs S10 and s11) for (a) 10  $\mu\text{m}$  and (b) 500 nm colloids at various ionic strength (note the difference in plot scales). Colloid zeta potential: -40 mV; and collector zeta potential: -40 mV.

## References

1. Duffadar, R. D.; Davis, J. M. *J. Colloid Interface Sci.* **2007**, *308*(1), 20-29.
2. Duffadar, R. D.; Davis, J. M. *J. Colloid Interface Sci.* **2008**, *326*(1), 18-27.
3. Bergendahl, J.; Grasso, D. *Chem. Eng. Sci.* **2000**, *55*(9), 1523-1532.
4. Johnson, K. L. *Contact Mechanics*. Cambridge University Press: Cambridge, UK, 1985.
5. Ma, H.; Pedel, J.; Fife, P.; Johnson, W. P. *Environ. Sci. Technol.* **2009**, *43*(22), 8573-8579.
6. Elimelech, M.; Gregory, J.; Jia, X.; Williams, R. A., *Particle Deposition and Aggregation: Measurement, Modeling and Simulation*. Butterworth-Heinemann: Boston, 1995.
7. Hogg, R.; Healy, T. W.; Fuerstenau, D. W. *Trans. Faraday Soc.* **1966**, *62*, 1638-1651.